JCTC Journal of Chemical Theory and Computation

Article

pubs.acs.org/JCTC

A Candidate Ion-Retaining State in the Inward-Facing Conformation of Sodium/Galactose Symporter: Clues from Atomistic Simulations

Ina Bisha,[†] Alessandro Laio,[†] Alessandra Magistrato,*[,‡] Alejandro Giorgetti,[¶] and Jacopo Sgrignani*[,‡]

[†]SISSA, Via Bonomea 265, 34165 Trieste, Italy

[‡]CNR-IOM-Democritos National Simulation Center c/o SISSA, via Bonomea 265, 34165 Trieste, Italy

[¶]University of Verona, Ca' Vignal 1, Strada Le Grazie 15, 37134 Verona, Italy

Supporting Information

ABSTRACT: The recent *Vibrio parahaemolyticus* sodium/galactose (vSGLT) symporter crystal structure captures the protein in an inward-facing substrate-bound conformation, with the sodium ion placed, by structural alignment, in a site equivalent to the Na2 site of the leucine transporter (LeuT). A recent study, based on molecular dynamics simulations, showed that the sodium ion spontaneously leaves its initial position diffusing outside vSGLT, toward the intracellular space. This suggested that the crystal structure corresponds to an ion-releasing state of the transporter. Here, using metadynamics, we identified a more stable Na^+ binding site corresponding to a putative ion-retaining state of the transporter. In addition, our simulations, consistently with mutagenesis studies, highlight the importance of D189 that, without being one of the Na^+-coordinating residues, regulates its binding/release.

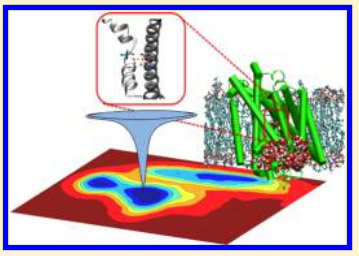

1. INTRODUCTION

Sodium-Galactose Transporter (SGLT) is a secondary active symporter, playing an important role in the accumulation of sugars (i.e., glucose or galactose) into cells, assuring the correct intestinal absorption and renal reabsorption.[1] Moreover, SGLT plays a very important role in water absorption as it can promote the uptake of about 6 L per day in a normal adult intestine. Despite the fact that the exact mechanism of water permeation is yet unclear,[1−3] this relevant function is exploited in the oral rehydration therapy (ORT) for the treatment of secretory diarrhea.[1,4]

SGLT belongs to the Sodium Solute Symporters (SSS) family, and, from the functional point of view, it uses the energy released as the sodium ion moves down its electrochemical gradient to power the 'uphill' movement of different substrates such as sugars, amino acids, vitamins, etc. The members of the SSS share two main features with the members of other gene families of Na^+-symporters: i.e. leucine transporter, LeuT, from Neurotransmitter Sodium Symporter (NSS) family, benzyl-hydantoin transporter, Mhp1, from Nucleobase Cation Symport (NCS1) family, betaine transporter, BetP, from Betaine Carnitine Choline (BCC) family, glutamate transporter, GltPh, from Excitatory Amino Acids Transporter (EAAT). The first common characteristic is the hypothesized transport cycle that occurs via an alternating-access mechanism[5,6] in which the protein switches from an outward to an inward-facing conformation. Second, despite their unrelated sequences, they have a common structural core of 10 transmembrane (TM) helices composed of two five-helix inverted repeat (5HIR) motifs. Thus, the investigation of the molecular mechanism of one of these proteins is important not only *per se* but also because it can provide information concerning the general mechanism of this class of secondary active transporters.

In recent years, the atomistic structures of several secondary symporters,[7−12] usually referred to as LeuT-fold proteins, have been solved by X-ray diffraction, providing insights into the molecular architecture of these transporters in the different stages of the transport cycle.[6] Many theoretical and experimental studies have been conducted on these structures, investigating the substrates releasing mechanism,[13−16] on the inward-outward conformational switch and on the investigation of the structural elements involved in a possibly general transport mechanism of the transporters sharing the LeuT-fold.[12,17−22]

Delicate issues concerning Na^+ ions in this type of transporters are as follows: (i) to locate the binding site of the Na^+ ion(s) and (ii) to understand their role along the transport mechanism. Recent studies addressed several ion-related aspects in the 5HIR proteins. Khafizov et al.,[23] for example, have recently employed MD simulations in parallel with experimental studies to characterize the Na^+-binding sites in BetP for which experimental evidence was lacking. Closer inspections of the role of the ions in Na1 and Na2 binding sites and in the dynamics of the transporters LeuT[24,25] and GltPh[16,25] have been also examined by theoretical studies. For this latter transporter also a third Na^+ binding site, not solved in the crystal structure, was identified.[26]

Concerning SGLT, in 2008 Faham et al.[9] reported the crystallization and structural resolution of this transporter from *Vibrio parahaemolyticus* bacterium (that shares the 32% of its sequence with the human homologue), capturing the protein in

Received: September 21, 2012
Published: January 2, 2013

the inward-facing occluded conformation. Even if the localization of the Na^+ ion binding site was not identified by the X-ray experiments, a plausible binding site was proposed by a structural comparison with the LeuT structure,[7] by considering the conservation of putative Na^+ binding residues among the SSS family and by mutational analysis.[9] However, recent molecular dynamics (MD) simulations studies suggested that the crystal structure represents an ion-releasing state of the transporter.[13,17,27] Indeed, starting from the binding site of the Na^+ ion proposed experimentally, after a few ns of MD simulation, the Na^+ spontaneously diffuses outside the protein, toward the intracellular space.

Here we focused on identifying a stable binding site for the ion in the inward-facing conformation, corresponding to a putative 'ion-retaining' state by performing classical MD and metadynamics (MTD)[28,29] simulations. Metadynamics (MTD) is a powerful method that allows exploring multidimensional free energy surfaces (FESs) by biasing the dynamics with a history-dependent potential. This enhances the probability of escaping from free-energy minima in which MD may remain trapped.[28,29] FES reconstruction is performed as a function of a few collective variables (CVs). In this case MTD was used to explore the FES and the conformations involved in the binding and dissociation of the Na^+ ion.

2. COMPUTATIONAL DETAILS

2.1. Model Building. The model of vSGLT was built using chain A of the 3.0 Å resolution crystal structure (PDB accession code 3DH4[9]). The first helix, solved only for the backbone atoms of residues S3−Y19, was eliminated, and it was then reconstructed taking these residues from a more recent crystal structure in which these residues were solved (PDB code 2XQ2,[17] 2.7 Å resolution). We did not choose this latter crystal as the starting structure of our simulations since it represents the inward-open ligands-free conformation of the transporter and, therefore, it was not useful for the aim of our study. (Note that in this paper we preferred to use the original numbering of the helices of the protein, i.e. from helix 1 to helix 14.[9]) The missing atoms of side chains of residues K124, V185, R273, K454, and K547 were reconstructed using SwissPDBViewer[30] application. All the Hys residues, far from the binding sites and oriented toward the solvent, were kept protonated in the ε position. The Asp and Glu residues were considered in the deprotonated form, while the Arg and Lys residues were considered in the protonated form. Residues S31 to L46, located between transmembrane helix (TM) 1 and TM2, and residues Y179 to A184, between TM5 and TM6, were constructed using the Loopy[31] program. This latter loop is far from the ion binding site and does not affect our results. The final monomeric structure contained 539 residues (S9 to K547). The protein was embedded in a pure, pre-equilibrated 1-palmitoyl-2-oleilphosphatidylcholine (POPC) lipid model (kindly supplied by T. A. Martinek)[32,33] using the g_membed[34] tool of Gromacs, and then it was oriented following the OPM[35] database model. Afterward the system was neutralized and solvated with the TIP3P model[36] water molecules (80969 total atoms in a box size of 97.6 × 96.7 × 85.1 $Å^3$). In Figure 1 is reported an overview of the whole simulated system.

2.2. Molecular Dynamics Simulations. Simulations were carried out with the GROMACS4[37] package using Amber03[38] force field for protein and GAFF[39] for membrane and galactose; for this latter, RESP[40] charges were calculated fitting an electrostatic potential calculated using the 6-31G* basis set and B3LYP[41,42] functional and the Gaussian03[43] program. The simulations were done in periodic boundary conditions at 310 K using the Nose-Hoover thermostat[44] and Parrinello-Rahman barostat[45,46] with a semisotropic pressure coupling type and a time step of 2 fs.

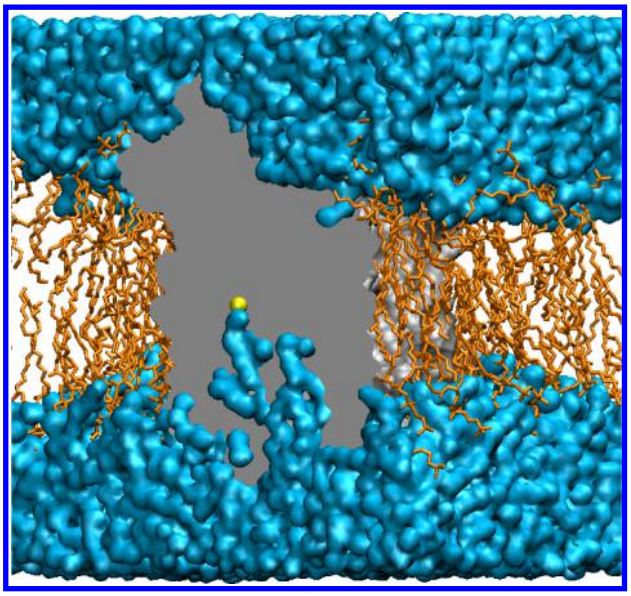

Figure 1. Overview of the simulated system. A section of vSGLT protein is shown in gray. From this view, the hydrophilic cavity of the protein, filled with many water molecules coming from the cytoplasmic side (the lower part of the figure with respect to the ion) is visible. The sodium ion in its binding site is colored in yellow. The POPC lipids are drawn in thick orange lines and water molecules in blue spheres.

Position restraints of atoms were fixed with a force constant (K) equal to 1000 kJ mol^{-1} nm^{-2}. Distance restraints were imposed using Umbrella Sampling keyword as implemented in Plumed[47] and considering the distances measured in the crystal structure as reference values and a K = 20000 kJ mol^{-1} nm^{-2}. The equilibration was performed in three stages: (1) The system was heated for 3 ns with protein backbone and ligands completely fixed, while side chains were left free to move. (2) 5 ns were run using distance restraints between the ligands and few close residues. These two stages were conducted in a NPγT ensemble with a surface tension equal to 600.0 bar*nm.[32] (3) Then the system was simulated for 26 ns where the membrane area was kept constant (Area Per Lipid around 64 $Å^2$).

Fifteen MD production runs of different lengths (one of 125 ns, 2 runs of 70 ns, 12 runs of 12 ns) were simulated. During all the simulations, we took care in particular that important parameters of the membrane, such as the Area Per Lipid (APL) and thickness, were in agreement with experimental values.[48]

2.3. Metadynamics Simulations. MTD was used in order to explore the FES and the conformations involved in the binding and dissociation of the Na^+ ion. Two different CVs were found to accurately describe this process: the coordination number of the ion with the carbonyl oxygens of A62, I65, and A361 and the hydroxyl oxygens (Oγ) of S364 and S365, the five closest residues in the crystal binding site, and the distance between Na^+ ion and the carboxylate group of D189. This latter is the only charged residue in the vicinity of the putative binding site, and it has been also previously observed to interact with the sodium ion along its exit pathway.[13,17] We remark that we considered also different sets of CVs (i.e., the water

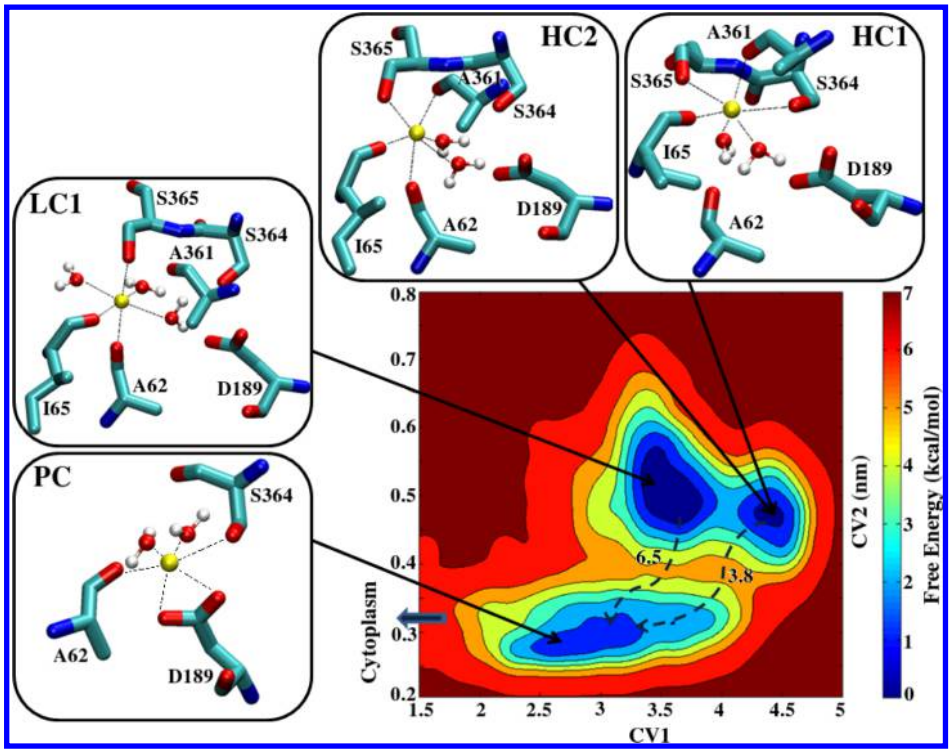

Figure 2. Free energy surface with the coordination states shown for the three minima. In the axes: CV1, the coordination number of the ion with the five closest residues in the crystal binding site (A62, I65, A361, S364, S365); CV2, the distance between Na^+ ion and D189. Anticlockwise boxes: the HC1 state, in which the ion interacts with residues I65 (on TM2), A361, S364 and S365 (on TM9); HC2 state, with residues I62 and A62 (on TM2), A361 and S365 (on TM9); both these states involve also two coordinating water molecules. Then the LC1 state, where the ion is coordinated by 3 residues (A62, I65, and S365) and 3 water molecules. The third minimum reports the PC state, coordinated by A62 and S364 from the crystal binding site, one or two Oδ of D189 and two water molecules. Except for the hydroxyl oxygens (Oγ) of the serines, the other residues coordinate the ion with carbonyl oxygens. The barriers on the path arrows are expressed in kcal/mol.

coordination of the Na^+ and the distance between two charged residues, D189-R273, that could have moved the two corresponding helices, TM6-TM7, closer to each other, making a saltbridge). However, the set previously described is the only one able to correctly describe the binding/release of Na^+ in a relatively short simulation time. Ten MTD simulations, of about 10 ns each, were performed using PLUMED 1.2[47] in the NVT ensemble. Gaussians width (ds) was 0.1 for CV1 and 0.02 nm for CV2, and the height (W) was equal to 0.4 kJ/mol for both CVs. The repulsive Gaussian potentials were added every 5 ps. These values were found to be optimal for the correct FES reconstruction.[29] To exactly estimate the exit barriers from the two most important minima determined by MTD we followed the procedure described in ref 29. Namely, we performed six independent MTD simulations starting from a configuration corresponding to different minima with initial velocities drawn at random from a Maxwell−Boltzmann distribution at 310 K. Then, we calculated the averages of the barriers and estimated the accuracy as the standard deviations of these values.

3. RESULTS AND DISCUSSION

3.1. Molecular Dynamics Simulations. After a careful setup of the system, we carried on an unbiased MD simulation aimed at elucidating the features of the experimental structure. We first analyzed the mechanism of water permeation.[1−3] Three different transport mechanisms have been proposed for this symporter: the water cotransport mechanism,[49,50] in which water is actively cotransported with Na^+ and glucose; the middle compartment hypothesis,[51] where solutes are transported developing local hypertonicity that drives water flux; and the local osmotic gradient hypothesis,[52] in which water molecules are transported passively through permeation pathway. Nevertheless, the last theoretical and experimental studies[3] support the passive mechanism. Consistently with these studies,[3] a visual inspection of our simulations shows that water molecules permeate relatively easily through the protein following a pathway[3] that presents a small gap of low water density localized in proximity of residues Y87 (on helix TM3), A259 (TM7), Q425 and Q428 (TM11), F479 and M483 (TM13).

We then verified whether the crystal structure of vSGLT represents an ion-releasing state of the transporter, consistent with the proposal of Li and Tajkhorshid.[27] Indeed, according to previous theoretical studies,[13,17,27] our simulation shows that Na^+ leaves its binding site in a few ns. In particular, initially the sodium ion interacts with D189, I65, and A62, but it loses its coordination with I65 after 1 ns. Then, it starts increasing its hydration (up to 3−4 water molecules). As it has been already shown for LeuT,[24] water molecules can penetrate from the cytoplasm into the protein core, entering through the hydrophilic cavity. This increases the local hydration of the Na^+ ion, probably facilitating its release from the Na2 site. In fact, after 6 ns, Na^+ exits the binding site. It moves toward the cytoplasm along TM9, passing close to the TM5-TM6 loop and finally exiting the protein after 12.5 ns. In order to evaluate the behavior of galactose we extended our simulation up to 125 ns. In spite of previous observations,[14,17] reporting spontaneous unbinding events of the substrate, in our case the galactose remained stably placed inside its binding site, conserving all its

starting interactions (see the Supporting Information (SI), Binding Sites section).

3.2. Metadynamics Simulations. To investigate which residues form a stable sodium binding site and affect ion specificity in the ion-occluded state of vSGLT, we performed six independent MTD simulations.

The free energy landscape explored is similar in all the independent metadynamics simulations (Figure 2). There are three distinguishable minima. Two minima correspond to high values of CVs, and they are close to each other. The third one, corresponding to lower values of CVs, is located far from the first two, and it is separated from them by a high barrier. By a cluster analysis, performed on all the MTD trajectories, in the regions corresponding to the three minima of the FES, we identified three putative binding states. All these states show the expected octahedral coordination for the Na^+ ion (Table 1).

Table 1. Protein Residues Included in the Coordination Sphere of Na^+ in the Four Different Coordination States (HC1, HC2, LC1, and PC) Identified Analyzing the MTD Simulations

	residues						
states	A62	I65	A361	S364	S365	D189	WAT
HC1		X	X	X	X		2
HC2	X	X	X		X		2
LC1	X	X			X		3
PC	X			X		X	2

For the sake of clarity, the different binding states were classified according to the coordinating residues. The first two states show a Na^+ ion coordinated by 4 residues and 2 water molecules. In particular, the first state (hereafter named Highly Coordinated 1 or HC1) involves residues I65 (on TM2), A361, S364, and S365 (on TM9); in the second state (hereafter named Highly Coordinated 2 or HC2) Na^+ interacts with I62 and A62 (on TM2) and A361 and S365 (on TM9). The chosen CVs cannot distinguish between HC1 and HC2, which correspond to the same minimum of the FES. Except for the hydroxyl oxygens (Oγ) of the serines, the other residues coordinate the ion with the oxygens of their carbonylic moieties. The coordinating distances Na^+-O are in the range of 2.3−2.7 Å, in good agreement with the experimental data of ion binding sites of LeuT and other ion channels or transporters[7,53] (see Table 2). Instead, the Na^+-O distances in the crystallografic structure of vSGLT (PDB code 3DH4) are significantly larger, in the range 3.1−3.6 Å (see Table 2). This is consistent with the hypothesis that the experimental structure corresponds to an ion-releasing state.

Another important minimum (hereafter Low Coordinated 1 or LC1) corresponds to a configuration where the ion is coordinated by 3 residues and 3 water molecules (3 + 3). The residues forming the coordination shell are A62, I65, and S365, and they bind to Na^+ with the carbonyl oxygens of A62 and I65 and hydroxyl oxygen of S365, as in HC1 and HC2. In this state the coordination distances Na^+-O are in the range of 2.3−2.6 Å, marginally smaller than in HC1-2. The three coordinated water molecules exchange with other waters during the simulation. Moreover, one of them makes simultaneously a H-bond with Na^+ and D189.

The third minimum, visible in Figure 2, shows the Na^+ ion poorly coordinated by protein residues (A62 and S364 forming the binding site hypothesized on the base of the crystal structure and also one or two Oδ of D189, close to the exiting pathway). This minimum (called hereafter Poorly Coordinated or PC) is quite close to the hydrophilic cavity opened toward the cytoplasm, formed from the intracellular portions of helices TM2, TM3, TM4, TM7, TM9, and TM11 (Figure S1). Therefore, it was not considered as a good ion-retaining candidate. Indeed, MD simulations started from this site unavoidably lead to the release of Na^+ in the cytoplasm.

3.3. Validation of Metadynamics Simulations. This FES in Figure 2 has been obtained by metadynamics with a bias acting on two variables, ending the simulation as soon as the

Table 2. Distances (Expressed in Å) for Sodium Binding Sites in the Crystal Structures of Several Na^+ Symporters[c]

symporter	PDB code	cystallographic distances between Na^+ ion and coordinating ligands				
vSGLT	3DH4	A62 (O)	I65 (O)	S365 (Oγ)	A361 (O)	S364 (Oγ)
		3.72	3.33	3.64	3.15	3.10
vSGLT[a]	**this work**	**A62 (O)**	**I65 (O)**	**S365 (Oγ)**		
		2.42 (±0.12)	**2.35 (±0.09)**	**2.62 (±0.19)**		
LeuT[b]	2A65	A22 (O)	N27 (Oδ)	T254 (Oγ)	T254 (O)	N286 (Oδ)
(Na1)		2.11	2.18	2.28	2.39	2.54
LeuT	2A65	G20 (O)	V23 (O)	A351 (O)	T354 (Oγ)	S355 (Oγ)
(Na2)		2.21	2.11	2.25	2.21	2.32
GltPh	2NWX	G306 (O)	N310 (O)	N401 (O)	D405 (Oδ1)	D405 (Oδ2)
(Na1)		2.70	2.61	2.73	2.71	2.77
GltPh	2NWX	T308 (O)		S349 (O)	T352 (O)	
(Na2)		2.75		1.96	2.48	
Mhp1		A38 (O)	I41 (O)	A309 (O)	S312 (Oγ)	T313 (Oγ)
(Na2)	2JLN (out)	2.62	2.66	2.09	2.53	2.77
	2JLO (occl)	2.84	2.79	2.56	2.62	2.65
	2X79 (inw)	residues far apart from each other, no ion				
BetP	4AIN	A147 (O)	M150 (O)	F464 (O)	T467 (Oγ)	S468 (Oγ)
(Na2)		2.17	2.48	2.33	2.31	2.36

[a]The three coordinating water molecules are not reported. [b]The sixth coordinating ligand in LeuT Na1 site is represented by the substrate, Leu (2.52 Å). [c]Except for vSGLT, we report the residues identified in the crystal structures within 3 Å from the ion. For vSGLT we report (in bold) also the average distances and standard deviations of the coordinating residues.

Na^+ ion reached the cytoplasm, well before the dynamics in CV space becomes diffusive.[29] In these conditions the FES obtained by metadynamics is accurate for what concerns the position of the free energy minima[28] but not for their relative depth and the height of the barriers. Thus, to determine exactly the barrier to exit the most important minima (HC1-2 and LC1) we followed the procedure described in ref 29. Namely, we performed three MTD simulations starting both from HC1 and LC1, assigning different initial velocities (see Computational Details).

The barrier that Na^+ has to overcome to leave the HC1 or HC2 sites toward the exiting PC site is of 3.8 (±0.4) kcal/mol; the exit pathway of the ion from these sites does not involve a passage from LC1. It involves a transient interaction with A62, S364, S365, and D189 and two water molecules (i.e., PC ligands plus S365), and it ends directly in the PC site, after losing the coordination with S365. The exit barrier from LC1 is significantly higher: 6.5 (±0.4) kcal/mol. The exit pathway from LC1 also ends directly in PC, without passing through HC1-2. These results suggest that LC1, despite its lower Na^+-protein coordination, is marginally more stable than HC1-2, leading to the consideration that this site is a more stable ion-retaining state than the one proposed on the basis of the crystal structure and bioinformatics analysis. We are aware that with our metadynamics simulations we performed only an exploration of the FES relative to small structural rearrangements of the residues surrounding the binding site. This does not rule out the existence of other Na^+ binding sites more stable than the one we identified in this work, which may require larger conformational changes with respect to the initial structure.

In order to further validate this prediction, considering that multiple short MD simulations enable a better exploration of the conformational space with respect to a single long simulation,[54] we performed 14 independent unbiased MD runs starting from different configurations and monitoring the conformational states explored by the dynamics. In seven simulations (4 performed starting from HC1 and 3 from HC2), the Na^+ ion, after spending a few nanoseconds on the HC2 state, moves to LC1 and remains in this configuration for the entire simulation time (12 ns). The variation of the CVs values during one of these simulations and their dependence on time have been reported in Figure S2. In two additional simulations, starting from LC1, the ion remains in that configuration for 70 ns without observing any modification (Table 2 and Figure S3). The last five runs, two started from HC1 and the other three from HC2, quickly lead the ion to interact with D189 and to the loss of its original coordinating ligands in a few ns. These observations confirm that HC1 and HC2, despite a larger protein coordination number, are marginally less stable than LC1. The barrier we find to escape from this site is consistent with the literature data of other symporters.[3,25,26,55,56] Indeed, the free energy barrier for the Na^+ dissociation from Na1 site in LeuT has been recently estimated to range between 14 and 6 kcal/mol,[25] depending on the extent of outward open conformation of the transporter. Interestingly, the minimal value of this barrier is consistent with our results. The binding affinities calculated recently for the ion in the Na1 site of GltPh are also consistent with our hypothesis.[26] Moreover, our values are in line also with the barriers estimated for ion conduction via membrane proteins estimated in computational studies.[55,56] Indeed, theoretical studies conducted on the X-ray structure of the KcsA K^+ channel showed that the largest free energy barrier for the process of ion conduction is on the order of 2−3 kcal/mol.[55] Similar values were found also by Furini et al.[56] in a theoretical work aimed at studying the conduction of Na^+ in bacterium Sodium Channel.

3.4. Final Remarks. The three binding states for the Na^+ ion identified in this work (HC1-2, LC1) share the interaction with the hydroxyl oxygen (Oγ) of S365 on TM9. Remarkably, this residue is conserved throughout the SSS family. Most importantly, mutation S365A leads to a complete abrogation of Na^+-dependent transport.[9]

Comparing the crystal structure of vSGLT and the protein conformation assumed when the Na^+ ion is in the LC1 state, we could not find any relevant difference in the orientation of the helices. However, we noted that, when Na^+ is in LC1, D189 is closer to the binding site with respect to the position occupied in the crystal structure (Figure 3). This conformation

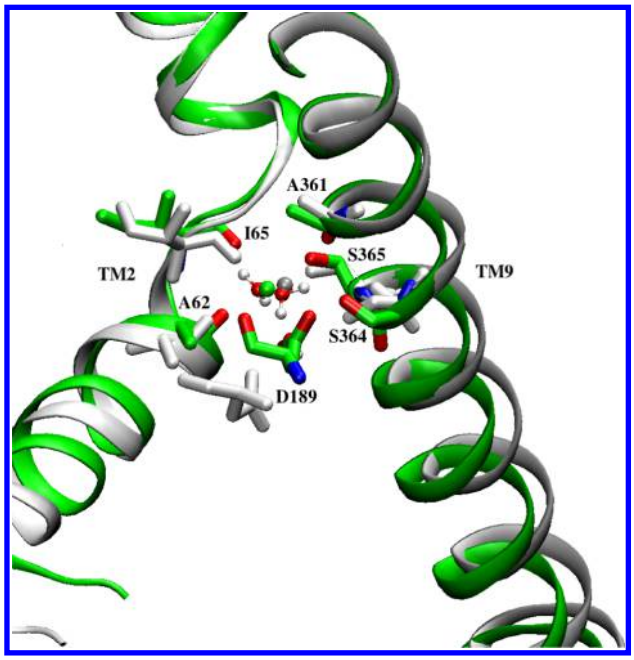

Figure 3. Overlap of crystal structure, colored in light gray, and LC1 conformation, in green. The most notable difference concerns the position of residue D189, much closer to the binding site in LC1.

is stabilized by a hydrogen bond with S364 (Oγ). Moreover, a water bridge between Na^+ and D189 is present both in LC1 and HC1-2. In addition, in the simulations where the Na^+ was unstable we observed a rotation of D189 toward the hydrophilic cavity that seems to be related with the exit of the ion. This residue is highly conserved throughout the SSS family, and experimental studies have highlighted its importance in a correct Na^+-galactose cotransport and in the cation selectivity.[57,58] Therefore, we hypothesize that D189 plays an important role in stabilizing the ion-retaining LC1 state.

Finally, molecular mechanics simulations strongly depend on the force field parameters especially when metal ions are considered.[59,60] To test the dependence of our results on the ion force field adopted,[38] we repeated one MTD simulation considering the ion force field parameters developed by Cheatham and co-workers.[61] Also in this case, we found results (the same free energy picture with the three minima containing the binding states described previously) similar to the other

MTD simulations. This excludes a strong influence of the force field parameters on the FES.

4. SUMMARY AND CONCLUSIONS

In the last years several efforts have been done to investigate the ion binding sites of the LeuT-fold secondary active transporters.[16,23−26] In this study we identified a putative ion-retaining state of vSGLT,[9,17] which is more stable than the one proposed on the basis of the crystal structure and bioinformatics considerations and mutational studies.[9,17] In fact, several theoretical works performed on this transporter showed a spontaneously diffusing ion outside the protein, leading to the hypothesis that the crystal structure represents an ion-releasing state of vSGLT.[13,17,27] By performing force field based MD and MTD simulations we identified the LC1 binding site, a site in which the Na^+ ion has an octahedral coordination geometry with three water molecules and three residues A62, I65 (carbonyl oxygens), and S365 (hydroxyl oxygen) forming its coordination shell. This state turns out to be stable for long (70 ns) MD simulations and is characterized by a barrier of approximately 6 kcal/mol to leave the coordination site. The coordination distances (Table 2, Figure S3) and the calculated barrier that the Na^+ ion has to overcome to exit from this minimum are consistent with the literature data.[3,25,26,55,56] The identification of this stable, ion-retaining binding site is very important not only for better understanding the mechanism of this symporter but also for identifying the sodium binding site in other 5HIR members for which crystallographic evidence is not available. Furthermore, this binding site could be important also for future inward-outward conformational change studies, whose structural elucidation is an important step to understand the transport mechanism of SGLT and other sodium symporters. In fact, describing the transport mechanism of vSGLT may allow for the formulation of the hypothesis on the general mechanism of other LeuT-fold transporters and of their eukaryotic analogues, sharing the same structural core domain of five helix inverted repeats. This may allow for the elucidation of the molecular mechanisms of several human diseases and provide the basis for a rational drug design of ligands that can control the regulation of those symporters.

■ ASSOCIATED CONTENT

Supporting Information

Details about galactose binding site; one figure representing the hydrophilic cavity; a panel reporting the variation of CV1 and CV2 in MD; one figure showing distances of the ion from the coordinating residues of the binding site in LC1. This material is available free of charge via the Internet at http://pubs.acs.org.

■ AUTHOR INFORMATION

Corresponding Author

*E-mail: alessandra.magistrato@sissa.it (A.M.); jacopo.sgrignani@icrm.cnr.it (J.S.).

Notes

The authors declare no competing financial interest.

■ ACKNOWLEDGMENTS

We acknowledge the CINECA award N. HP10BTNWLY, 2011, for the availability of high performance computing resources and support.

■ REFERENCES

(1) Wright, E. M.; Loo, D. D.; Hirayama, B. A. *Physiol. Rev.* **2011**, *91*, 733−794.
(2) Choe, S.; Rosenberg, J.; Abramson, J.; Wright, E.; Grabe, M. *Biophys. J.* **2010**, *99*, L56−L58.
(3) Sasseville, L.; Cuervo, J.; Lapointe, J.; Noskov, S. *Biophys. J.* **2011**, *101*, 1887−1895.
(4) Wright, E.; Hirayama, B.; Loo, D. *J. Intern. Med.* **2007**, *261*, 32−43.
(5) Jardetzky, O. *Nature* **1966**, *211*, 969−970.
(6) Abramson, J.; Wright, E. M. *Curr. Opin. Struct. Biol.* **2009**, *19*, 425−432.
(7) Yamashita, A.; Singh, S. K.; Kawate, T.; Jin, Y.; Gouaux, E. *Nature* **2005**, *437*, 215−223.
(8) Weyand, S.; Shimamura, T.; Yajima, S.; Suzuki, S.; Mirza, O.; Krusong, K.; Carpenter, E.; Rutherford, N.; Hadden, J.; O'Reilly, J.; et al. *Science's STKE* **2008**, *322*, 709.
(9) Faham, S.; Watanabe, A.; Besserer, G. M.; Cascio, D.; Specht, A.; Hirayama, B. A.; Wright, E. M.; Abramson, J. *Science* **2008**, *321*, 810−814.
(10) Ressl, S.; van Scheltinga, A.; Vonrhein, C.; Ott, V.; Ziegler, C. *Nature* **2009**, *458*, 47−52.
(11) Yernool, D.; Boudker, O.; Jin, Y.; Gouaux, E. *Nature* **2004**, *431*, 811−818.
(12) Perez, C.; Koshy, C.; Yildiz, Ö.; Ziegler, C. *Nature* **2012**, *490*, 126−130.
(13) Zomot, E.; Bahar, I. *Mol. Biosyst.* **2010**, *6*, 1040−1046.
(14) Li, J.; Tajkhorshid, E. *Biochim. Biophys. Acta* **2012**, *1818*, 263−271.
(15) Gu, Y.; Shrivastava, I.; Amara, S.; Bahar, I. *Proc. Natl. Acad. Sci. U.S.A.* **2009**, *106*, 2589−2594.
(16) Grazioso, G.; Limongelli, V.; Branduardi, D.; Novellino, E.; De Micheli, C.; Cavalli, A.; Parrinello, M. *J. Am. Chem. Soc.* **2011**, *134*, 453−463.
(17) Watanabe, A.; Choe, S.; Chaptal, V.; Rosenberg, J. M.; Wright, E. M.; Grabe, M.; Abramson, J. *Nature* **2010**, *468*, 988−991.
(18) Forrest, L.; Rudnick, G. *Physiology* **2009**, *24*, 377−386.
(19) Shimamura, T.; Weyand, S.; Beckstein, O.; Rutherford, N.; Hadden, J.; Sharples, D.; Sansom, M.; Iwata, S.; Henderson, P.; Cameron, A. *Science* **2010**, *328*, 470−473.
(20) Weyand, S.; Shimamura, T.; Beckstein, O.; Sansom, M.; Iwata, S.; Henderson, P.; Cameron, A. *J. Synchrotron Radiat.* **2010**, *18*, 20−23.
(21) Shaikh, S.; Tajkhorshid, E. *PLoS Comput. Biol.* **2010**, *6*, e1000905.
(22) Adelman, J.; Dale, A.; Zwier, M.; Bhatt, D.; Chong, L.; Zuckerman, D.; Grabe, M. *Biophys. J.* **2011**, *101*, 2399−2407.
(23) Khafizov, K.; Perez, C.; Koshy, C.; Quick, M.; Fendler, K.; Ziegler, C.; Forrest, L. *Proc. Natl. Acad. Sci. U.S.A.* **2012**, *109*, E3035−E3044.
(24) Zhao, C.; Noskov, S. *Biochemistry* **2011**, *50*, 1848−1856.
(25) Zhao, C.; Stolzenberg, S.; Gracia, L.; Weinstein, H.; Noskov, S.; Shi, L. *Biophys. J.* **2012**, *103*, 878−888.
(26) Bastug, T.; Heinzelmann, G.; Kuyucak, S.; Salim, M.; Vandenberg, R.; Ryan, R. *PLoS One* **2012**, *7*, e33058.
(27) Li, J.; Tajkhorshid, E. *Biophys. J.* **2009**, *97*, 29−31.
(28) Laio, A.; Parrinello, M. *Proc. Natl. Acad. Sci. U.S.A.* **2002**, *99*, 12562−12566.
(29) Laio, A.; Gervasio, F. *Rep. Prog. Phys.* **2008**, *71*, 126601.
(30) Guex, N.; Peitsch, M. C. *Electrophoresis* **1997**, *18*, 2714−2723.
(31) Xiang, Z.; Soto, C. S.; Honig, B. *Proc. Natl. Acad. Sci. U.S.A.* **2002**, *99*, 7432−7437.
(32) Jójárt, B.; Martinek, T. A. *J. Comput. Chem.* **2007**, *28*, 2051−2058.
(33) Sgrignani, J.; Magistrato, A. *J. Chem. Inf. Model.* **2012**, *52*, 1595−1606.
(34) Wolf, M. G.; Hoefling, M.; Aponte-Santamaría, C.; Grubmüller, H.; Groenhof, G. *J. Comput. Chem.* **2010**, *31*, 2169−2174.
(35) Lomize, M. A.; Lomize, A. L.; Pogozheva, I. D.; Mosberg, H. I. *Bioinformatics* **2006**, *22*, 623−625.

(36) Mahoney, M.; Jorgensen, W. *J. Chem. Phys.* **2000**, *112*, 8910.
(37) Hess, B.; Kutzner, C.; Van Der Spoel, D.; Lindahl, E. *J. Chem. Theory Comp.* **2008**, *4*, 435−447.
(38) Duan, Y.; Wu, C.; Chowdhury, S.; Lee, M.; Xiong, G.; Zhang, W.; Yang, R.; Cieplak, P.; Luo, R.; Lee, T.; et al. *J. Comput. Chem.* **2003**, *24*, 1999−2012.
(39) Wang, J.; Wolf, R.; Caldwell, J.; Kollman, P.; Case, D. *J. Comput. Chem.* **2004**, *25*, 1157−1174.
(40) Bayly, C.; Cieplak, P.; Cornell, W.; Kollman, P. *J. Phys. Chem.* **1993**, *97*, 10269−10280.
(41) Lee, C.; Yang, W.; Parr, R. *Phys. Rev. B* **1988**, *37*, 785.
(42) Stephens, P.; Devlin, F.; Chabalowski, C.; Frisch, M. *J. Phys. Chem.* **1994**, *98*, 11623−11627.
(43) Frisch, M.; Trucks, G.; Schlegel, H.; Scuseria, G.; Robb, M.; Cheeseman, J.; Montgomery, J., Jr.; Vreven, T.; Kudin, K.; Burant, J.; et al. Gaussian Inc.: Wallingford, CT, 2004.
(44) Evans, D.; Holian, B. *J. Chem. Phys.* **1985**, *83*, 4069.
(45) Parrinello, M.; Rahman, A. *J. Appl. Phys.* **1981**, *52*, 7182−7190.
(46) Nose, S.; Klein, M. *Mol. Phys.* **1983**, *50*, 1055−1076.
(47) Bonomi, M.; Branduardi, D.; Bussi, G.; Camilloni, C.; Provasi, D.; Raiteri, P.; Donadio, D.; Marinelli, F.; Pietrucci, F.; Broglia, R.; et al. *Comput. Phys. Commun.* **2009**, *180*, 1961−1972.
(48) Kučerka, N.; Tristram-Nagle, S.; Nagle, J. *J. Membr. Biol.* **2006**, *208*, 193−202.
(49) Loo, D.; Wright, E.; Zeuthen, T. *J. Physiol.* **2004**, *542*, 53−60.
(50) Zeuthen, T.; Meinild, A.; Loo, D.; Wright, E.; Klaerke, D. *J. Physiol.* **2004**, *531*, 631−644.
(51) Naftalin, R. *Curr. Opin. Chem. Biol. Biophys. J.* **2008**, *94*, 3912−3923.
(52) Duquette, P.; Bissonnette, P.; Lapointe, J. *Proc. Natl. Acad. Sci. U.S.A.* **2001**, *98*, 3796−3801.
(53) Harding, M. *Acta Crystallogr., Sect. D: Biol. Crystallogr.* **2002**, *58*, 872−874.
(54) Evanseck, J.; Caves, L.; Karplus, M. *Protein Sci.* **1998**, *7*, 649−666.
(55) Berneche, S.; Roux, B. *Nature* **2001**, *414*, 73−76.
(56) Furini, S.; Domene, C. *PLoS Comput. Biol.* **2012**, *8*, e1002476.
(57) Quick, M.; Loo, D.; Wright, E. *J. Biol. Chem.* **2001**, *276*, 1728−1734.
(58) Quick, M.; Jung, H. *Biochemistry* **1998**, *37*, 13800−13806.
(59) Zimmer, M. *Coord. Chem. Rev.* **2009**, *253*, 817−826.
(60) Sgrignani, J.; Pierattelli, R. *J. Biol. Inorg. Chem.* **2012**, *17*, 71−79.
(61) Joung, I. S.; Cheatham, T. E. *J. Phys. Chem. B* **2008**, *112*, 9020−9041.